Vysoké učení technické v Brně
Fakulta chemická
Purkyňova 464/118, 61200 Brno

Zadání bakalářské práce

Číslo bakalářské práce:	**FCH-BAK0946/2015**	Akademický rok:	**2015/2016**
Ústav:	Ústav chemie materiálů		
Student(ka):	**Barbora Bella Klepáčková**		
Studijní program:	Chemie a chemické technologie (B2801)		
Studijní obor:	Chemie, technologie a vlastnosti materiálů (2808R016)		
Vedoucí práce	**prof. RNDr. Vladimír Čech, Ph.D.**		
Konzultanti:			

Název bakalářské práce:

Volná povrchová energie plazmových polymerů

Zadání bakalářské práce:

-Literární rešerše z oblasti plazmochemické depozice z plynné fáze, měření smáčivosti a stanovení volné povrchové energie.
-Praktické zvládnutí měření kontaktních úhlů a vyhodnocení volné povrchové energie.
-Měření kontaktních úhlů pro vybrané vrstvy plazmových polymerů.
-Posouzení vztahu volné povrchové energie a depozičních podmínek.

Termín odevzdání bakalářské práce: 20.5.2016

Bakalářská práce se odevzdává v děkanem stanoveném počtu exemplářů na sekretariát ústavu a v elektronické formě vedoucímu bakalářské práce. Toto zadání je přílohou bakalářské práce.

Barbora Bella Klepáčková Student(ka)	prof. RNDr. Vladimír Čech, Ph.D. Vedoucí práce	prof. RNDr. Josef Jančář, CSc. Ředitel ústavu

V Brně, dne 31.1.2016

prof. Ing. Martin Weiter, Ph.D.
Děkan fakulty

BRNO UNIVERSITY OF TECHNOLOGY
VYSOKÉ UČENÍ TECHNICKÉ V BRNĚ

FACULTY OF CHEMISTRY
FAKULTA CHEMICKÁ

INSTITUTE OF MATERIALS SCIENCE
ÚSTAV CHEMIE MATERIÁLŮ

SURFACE FREE ENERGY OF PLASMA POLYMERS
VOLNÁ POVRCHOVÁ ENERGIE PLAZMOVÝCH POLYMERŮ

BACHELOR'S THESIS
BAKALÁŘSKÁ PRÁCE

AUTHOR — Barbora Bella Klepáčková
AUTOR PRÁCE

SUPERVISOR — prof. RNDr. Vladimír Čech, Ph.D.
VEDOUCÍ PRÁCE

BRNO 2016

ABSTRACT

Changes of free surface energy of organosilicon plasma polymers according to their different deposition conditions were studied in this thesis. The free surface energy was evaluated using the Owens-Wendt-Kaelble, Wu and acid-base theory. Four different test liquids were used to determine contact angles (water, form amide, diiodomethane and glycerol). Measuring tetravinylsilane thin films with effective power of 2, 10, 25, 70 and 150 W showed a slightly increasing surface free energy.

ABSTRAKT

Tato práce se zabývá studiem změn volné povrchové energie organokřemičitých plasmových polymerů na základě jejich rozdílných depozičních podmínek. Výpočet volné povrchové energie byl proveden pomocí Owens-Wendt-Kaelble, Wu a acido-bazické teorie. K měření kontaktních úhlů bylo použito čtyř různých testovacích kapalin (voda, formamid, dijodmethan a glycerol). Pro tenké vrstvy plasmového tetravinylsilanu připraveného s efektvním výkonem 2, 10, 25, 70 a 150 W byla naměřená volná povrchová energie mírně vzrůstající.

KEYWORDS

plasma polymers, organosilicons, wettability, surface free energy, contact angle

KLÍČOVÁ SLOVA

plazmové polymery,organokřemičitany, smáčivost, volná povrchová energie, kontaktní úhel

BIBLIOGRAPHICAL CITATION

KLEPÁČKOVÁ, B. B. *Volná povrchová energie plazmových polymerů.* Brno: Vysoké učení technické v Brně, Fakulta chemická, 2016. 37 s. Vedoucí bakalářské práce prof. RNDr. Vladimír Čech, Ph.D.

DECLARATION

I declare that the bachelor thesis has been worked out by myself and that all the quotations from the used literary sources are accurate and complete. The content of the bachelor thesis is the property of the Faculty of Chemistry of Brno University od Technology and all commercial uses are allowed only if approved by both the supervisor and the dean of the Faculty of Chemistry, BUT.

.....

student‘s signature

ACKNOWLEDGMENT

First I would like to thank my family for persuading me not to give up anytime. Then my acknowledgement goes to prof. RNDr. Vladimír Čech, Ph.D. for his help and mentoring.

This work was supported in part by the Technology Agency of the Czech Republic, grant no. TA01010796, and the Czech Science Foundation, grant no. 16-09161S.

CONTENTS

INTRODUCTION 5

2 THEORETICAL PART 6

2.1 Plasma polymerization 7

2.1.1 Mechanism 8

2.1.2 Deposition conditions 9

2.1.3 Plasma polymers of organosilicones 10

2.2 Surface wettability 11

2.2.1 Measurement methods 12

2.2.2 Surface free energy 14

3 EXPERIMENTAL PART 17

3.1 Tested plasma polymers 17

3.1.1 Deposition conditions 17

3.2 Contact angle measurements 18

3.2.1 Used device 18

3.2.2 Measurement procedure and calculation 18

4 RESULTS AND DISCUSSION 21

5 CONCLUSION 31

6 LIST OF SOURCES 32

7 LIST OF ABBREVIATIONS AND SYMBOLS 36

INTRODUCTION

Let me introduce some basic facts about materials which are discussed in this thesis at the beginning. Organosilicon molecules consist of silicon atom in the backbone chain and organic groups in the rest two positions on a silicon atom. They are widely used in electro engineering for a coating on integrated circuits, in production of solar panels or in chemistry as a composite reinforcement modifier etc.

Also the usage of thin film polymers is quite common these days. Not just because it is expensive to produce big amounts of polymer materials but it has a lot of scientifically interesting properties and relations that can be observed. Even many branches of both science and industry develop really small components and their need of covering extremely small surfaces is increasing.

This bachelor's thesis focuses on measuring wettability of plasma polymer thin films by evaluation of contact angles of stable test liquids. The aim is to determine free surface energy of these materials by using three different theories of calculation. Also a dependence of free surface energy on deposition conditions is observed.

From my point of view, this topic seems to offer some interesting results of connection between the way the film was made and its wettability.

2 THEORETICAL PART

Thin films (also called layers or coatings) are defined as materials which two dimensions are extremely bigger than the third one. Usually the smallest dimension measure 0.1 nm–10 μm. Theoretically they are considered as two-dimensional objects and they have a negligible volume in comparison with their surface area (Fig. 1).

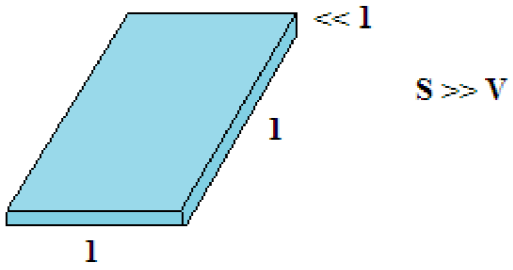

Fig. 1: A scheme of a thin film dimension

At the opposite there are bulk materials. Their properties are related to the volume unit. But properties and interactions of thin films with other substances differ from common bulk materials (Fig. 2). Atoms on surface of a layer are so close to each other so they influence mechanical, optical, electronic and thermal properties of a whole unit. They are also more likely to be influenced by interatomic potentials and surface energy than by macroscopic mechanical properties. [1]

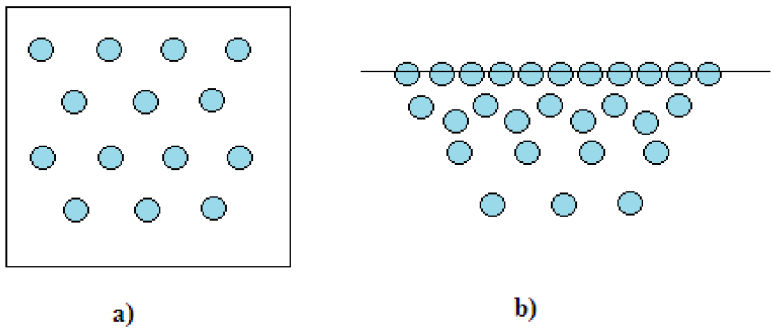

Fig. 2: A scheme of structure of **a)** bulk and **b)** thin film material

According to the size (or thickness) of a layer there is a classical or quantum dimensional phenomena. Classical dimensional phenomena can be observed in films where the thickness of a layer is comparable to the mean of electrons. Or in case of galvanometric phenomena there is a film comparable to the radius of electrons in magnetic field. Quantum dimensional phenomena can be observed in crystalline films where the film thickness is comparable to the Broglie wavelength of electron.

Many types of materials can form a thin film. They can be organic, inorganic or hybrid. They can have crystalline, semi crystalline or even an amorphous form. We can form glass, metal, polymer, ceramic and composite thin films in order to prepare an appropriate surface. When it comes to polymer surfaces in such a thin layer there is a connection between the adhesion and chemical bonds within the reinforcement material and polymer coating. [2] The bigger the adhesion of the interlayer occurs, the more stable and stronger the interface is. There are four types of bonds that can be observed on the surface: Van der Waals´ forces, electrostatic forces, structural forces and short-range interactions (i.e. hydrogen bonding). [3] We usually describe the strength of these interactions as the surface energy, surface tension or free surface energy.

2.1 Plasma polymerization

Plasma is a special state of matter (see Fig. 3) caused by providing substance a big amount of energy, e.g. heat, to initiate an ionization of atoms and molecules. In this state a mixture of protons, electrons, radicals and neutral atoms can be found in the gas phase. [4] Temperature, velocity and kinetic energy of involved particles lead to higher reactivity of atoms and molecules in the plasma exposed system because of interactions (i.e. collisions) between them. Also an electric field can be used for increasing the velocity of particles, if needed. There are three types of plasma – thermal, cold and hybrid. [5] Thermal plasma occurs if molecules, ions and electrons of gas reach the thermal equilibrium at high temperature (about thousands of Kelvin). Providing system enough energy to create cold plasma is usually done by electric generators under low pressure. [4] Finally hybrid plasma is produced by special devices such as ozonizer or corona discharger at normal temperature. [5]

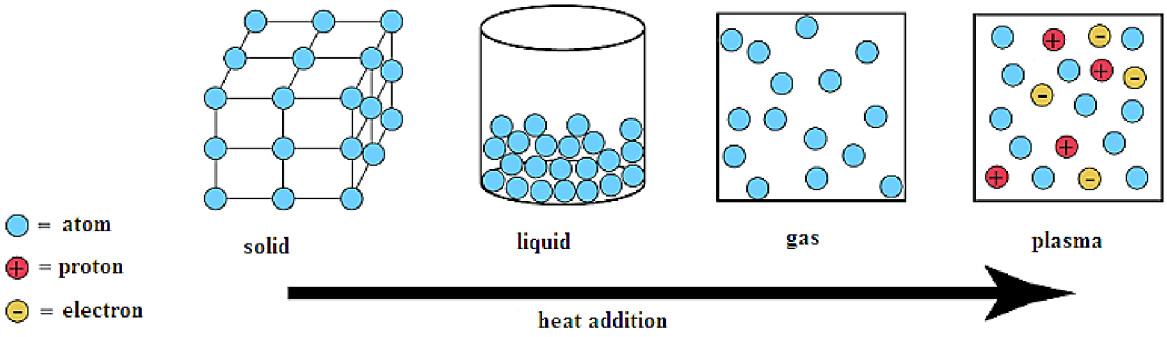

Fig. 3: A structure of all states of matter

For activating monomer units by plasma some organic gases like hydrocarbons or alkylsilanes are necessary. Plasma containing those substances is called as a polymer-forming. Otherwise plasma with inorganic gases like argon, helium, hydrogen, nitrogen and oxygen is called a non-polymer-forming plasma, because those gases cause etching reactions, implantation of atoms and radical generation instead. [4]

Plasma polymerization is special in a way that polymer product is produced. In common ionic or radical polymerization a whole monomer molecule reacts to form ion or radical. Then a propagation follows until none of monomer units is left or termination begins. Using plasma

for initiating a reaction causes decomposition of monomer into fragments when particles of plasma reach the decomposition energy of the particular monomer. A simple scheme is shown in the Fig. 4.

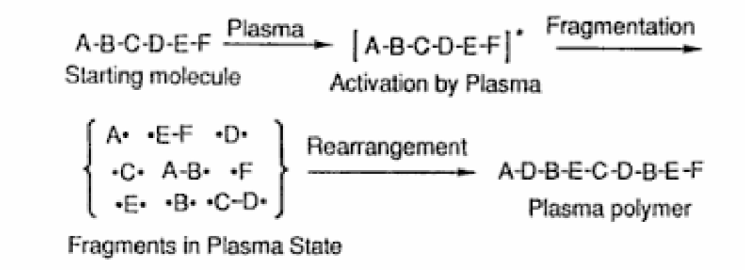

Fig. 4: A plasma polymerization scheme [4]

According to Inagaki (1996) we can distinguish two types of fragmentation reactions: the elimination of the hydrogen atom (at the Fig. 5) and C – C bond scission (Fig. 6).

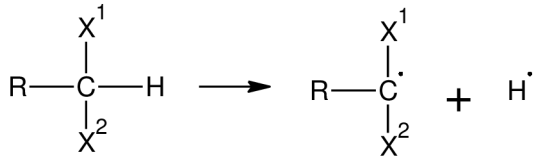

Fig. 5: Hydrogen elimination

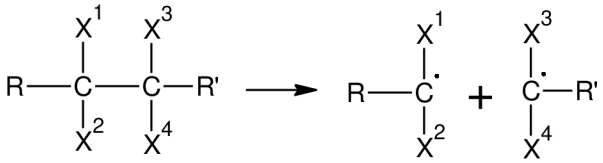

Fig. 6: C – C bond scission

Those parts recombine and create molecules with large molecular weight on the substrate surface or in gas phase. [4] Fragments on the surface are spread irregularly and individual monomer units cannot be distinguished. However, using appropriate monomer and deposition conditions a continuous thin film polymer with united features can be prepared. The advantage of plasma polymerized films is mainly their higher density. It exceeds conventional polymers produced by other processes.

2.1.1 Mechanism

The mechanism of plasma polymerization has a stepwise character (as can be seen at Fig. 7). It starts when a monomer molecule M_i looses its hydrogen atom it became a radical M_i• or with another hydrogen atom eliminated, a biradical •M_k•. Then there are three possibilities for each radical to recombine. First with monomer unit M to form longer chain radical or biradical molecules M_i-M• or •M_k-M•. Secondly with another radical of the same type (i.e. two radicals and two biradicals together) forming a new neutral molecule M_j-M_j, which undergoes the plasma activation and pass the cycle all over again, or at the other hand

forming a longer chain biradical •M_k-M_j•. All of radical products return in the cycle to the beginning and react again the same way. Finally those two different particles (radical and biradical) recombines together. So a completely new radical occurs •M_k-M_j and follows the reactions cycle again. Double and triple bond creating reactions of radicals M_i• and •M_k• occur just occasionally due to low ceiling (also critical) temperature where the reaction is in equilibrium between the polymerization and depolymerization. [4] This fact comes from the equation of the Gibbs free energy (1).

$$\Delta G = \Delta H - T\Delta S \qquad (1)$$

When the temperature T raises to the critical point T_c, the magnitude of $T\Delta S$ (S stands for entropy) increases and equals the value of enthalpy ΔH. Then the Gibbs free energy becomes zero and there is equilibrium within the system.

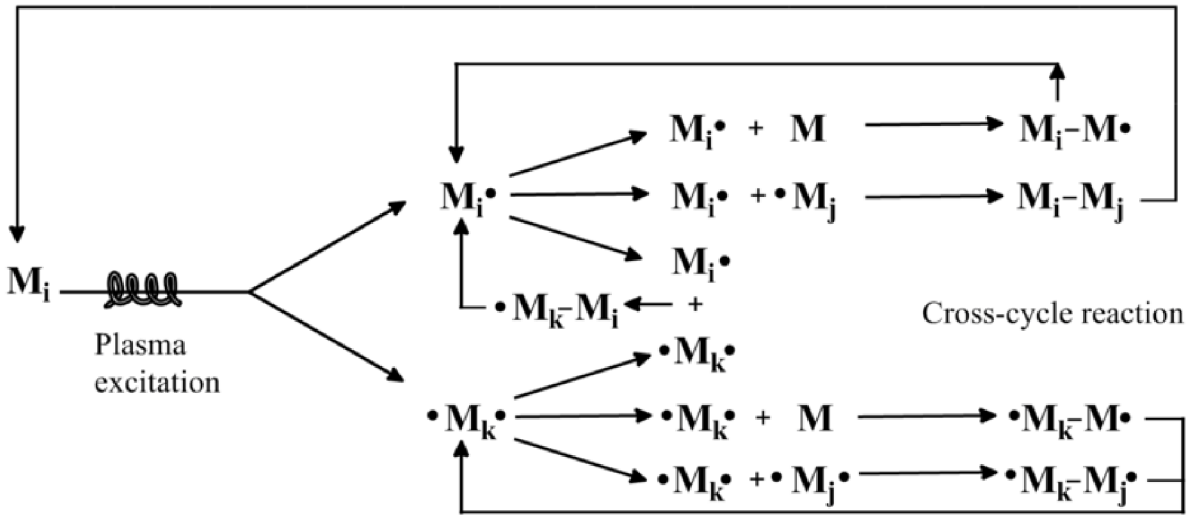

Fig. 7: A scheme of plasma polymerization mechanism [4]

2.1.2 Deposition conditions

During preparation of plasma polymer there are few factors influencing features of a final product. They are called deposition conditions. They are essentially for repeating the experiment the same way because there are evidences that different style of deposition produces polymer films of different features. First of them is the gas atmosphere. According to the gas used while producing polymer thin film, there are some differences on the polymer surface caused by bonding atoms of the gas with the surface polymer atoms. Then there is an effective power activating the plasma. It controls the deposition rate and determines the energy added to the rising polymer film. A result also affect deposition pressure, time and monomer flow rate. Time of deposition correlates to the thickness of film, lower pressure is necessary for evolving cold plasma. [6]

The activation of monomers and reactivation of the recombined molecules by plasma, as described earlier, are essentially due to fragmentation. This process depends on how much electric energy is provided to plasma (effective power). Thus when speaking about deposition

conditions, it is appropriate to mention the Yasuda parameter (Yasuda, H. 1973), too. It is a controlling parameter of *W/FM* value, where *W* is equal to the electric energy supplying plasma in J/s, *F* is the monomer flow rate in mol/s and *M* stands for the molecular weight of the monomer in kg/mol. The magnitude of Yasuda parameter (*W/FM)* is considered to be proportional to the concentration of activated species in plasma. So the polymer deposition rate increases together with increasing Yasuda parameter in system with lower activated species concentrations than the concentration of monomer molecules. Afterward the polymer deposition rate levels off and over the competition region, and decreases with increasing *W/FM* parameter because of lack of monomer molecules (monomer deficient region). [4]

2.1.3 Plasma polymers of organosilicons

Organosilicons belong to inorganic polymer compounds. They consist of at least one atom of silicon and organic groups where atoms of carbon, oxygen, nitrogen and hydrogen can be found. There are a lot of organosilicon monomers used to form plasma polymer thin films. Few of them are shown in a Tab. 1. These are the main commonly used monomer = precursors. [7]

Tab. 1: Main organosilicon precursors and conditions used to growth plasma films [7]

Name	Shortcut	Pressure range	Power range	Reference
Hexamethyldisiloxane	HMDSO	10^{-3} to 1 mbar	3–100 W	[8], [9], [10], [11], [12]
Tetraethoxysilane	TEOS	10^{-3} to 1 mbar	3–100 W	[13], [14], [15], [16]
Tetramethyldisiloxane	TMDSO	1,3 Pa	25 W	[17]
Divinyltetramethyldisiloxane	DVTMDSO	10^{-3}–10^{-1} mbar	14–200 W	[18]
Methyltrimethoxysilane	TMOS	0,110 Torr	300 W	[19]
Hexamethyldisilane	HMDS	1,3 Pa	50–150 W	[20]
Tetramethylsilane	TMS	1,3 Pa	25 W	[17]

The mostly used precursors are HMDSO and TEOS. These monomers are very often used in mixtures with a rare gas like Argon or an active gas (e. g. O_2, N_2O). It is generally admitted that the atomic oxygen is created, while using active gas, in the plasma phase and it reacts in the gas and at the plasma-surface interface with the organic parts of the monomer. Precursors HMDSO and TMDSO are very similar; they both contain at least one Si-O bond in their structure. However TMDSO presents the advantage of having a weak Si-H bond so it's easily dissociable. HMDS and TMS monomers does not contain any oxygen or nitrogen atom, thus addition of oxygenated or nitrogenized gas is necessary to obtain Si-O or Si-N bond in the deposited layer.

This thesis works with tetravinylsilane (TVS) (see Fig. 8) monomer. This polymer precursor also does not contain any oxygen or nitrogen atom. But, due to its tetravalent silicon, it can create a three-dimensional polymeric network. These properties are suitable for

using TVS plasma polymers as compatible interlayers in polymer composites with glass fibers.

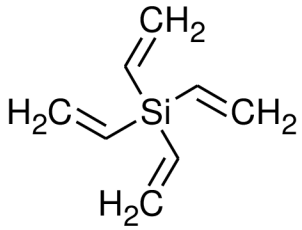

Fig. 8: A formula of tetravinylsilane (TVS)

2.2 Surface wettability

Wettability is an ability of liquid to adhere to the solid surface. It is equal to result of adhesive and cohesive forces between particles in the interface. This ability is for sure the most important for sticking two substances together, such as polymer matrix and reinforcement in polymer composite materials, or in our case fixing a polymer thin film to a glass or silicone substrate.

Cohesion work stands for the work required for separating reversibly one phase of liquid or solid in two parts with unit sectional area (2):

$$W_c = 2 \cdot \gamma_A . \tag{2}$$

Adhesion work is determined as the work needed for separating reversibly two phases (liquids *A* and *B*) from their equilibrium to infinity while the interface *AB* perishes and two new interfaces of separate *A* and *B* appears. This work is described with Dupré's equation (3):

$$W_a = \gamma_A + \gamma_B - \gamma_{AB}, \tag{3}$$

where W_a is the adhesion work, γ_A is the surface tension of liquid *A*, γ_B is the surface tension of liquid *B* and γ_{AB} is the surface tension of the interface between both liquids. [5]

For describing the wettability between solid and liquid, we usually use the contact angle θ. It's an angle of liquid drop (surrounded with gas) with the solid surface. This is also called the three-phase boundary (Fig. 9) and it's determined by Young equation (4):

$$\gamma_{LG} \cdot \cos\theta = \gamma_{SG} - \gamma_{LS}, \tag{4}$$

where γ_{LG} is the surface tension in equilibrium between liquid and surrounding gas, θ is the contact angle of liquid and solid, γ_{SG} is the surface tension in equilibrium between solid and gas and γ_{LS} is the surface tension in equilibrium between liquid and solid. [21]

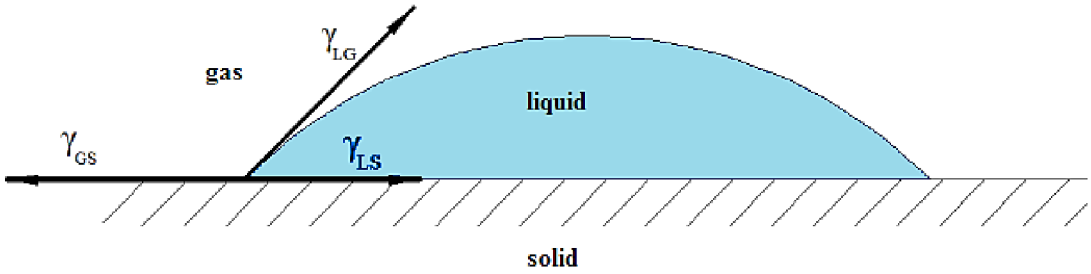

Fig. 9: Three-phase boundary

The higher the contact angle is the more is the liquid wettable. Absolutely non wettable liquids form a perfect drop on the surface. Absolutely wettable liquids form a very thin layer. On the Fig. 10 there are three kinds of liquid – good, bad and non wettable.

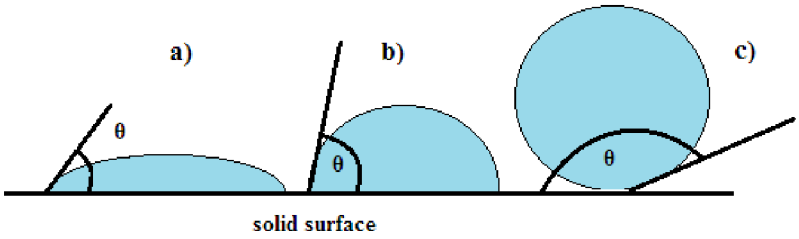

Fig. 10: Drops of liquid with **a)** high, **b)** lower and **c)** no wettability

When it comes to adhesion of liquid and solid, there is a Young-Dupré's equation (5) describing the relation between the contact angle θ and surface tension of solid-liquid interface γ_{SL}:

$$W_a = \gamma_{LS} \cdot (1 + \cos\theta). \tag{5}$$

This equation also leads to calculation of surface free energy.

2.2.1 Measurement methods

Measuring contact angles of a liquid-solid system can be done several ways. Drop-bubble methods use liquid drops (a sessile drop method) or air bubbles (captive bubble method) resting on plane solid surfaces. There are three possibilities how to measure individual contact angles. First is direct observation (or tangent) method. It concern measuring the angle between the tangents to the profile at the point of contact with the solid surface (see Fig. 10). The second is called reflected light method, where a light beam emitted from a microscope is reflected back when the microscope is focused on a three-phase contact point. However, disadvantage of this method is its validity only for angles less than 90°. The third method is utilized for measuring really small angles (about 10°) and is called interference microscopy method. There is a monochromatic light reflected with a beam splitter onto the reflecting substrate to form interference bands parallel to the drop edge. The contact angle is calculated

from the spacing of the interference bands, the refractive index of the liquid and the wavelength of the light. [5]

Wilhelmy plate (or tensiometric) method is suitable for measuring contact angle on flat plates or filaments. Calculation of force F_w on a thin plate (6) is related to the perimeter p, liquid surface tension γ, contact angle θ, the liquid density ρ, the gravitational acceleration g, the cross-sectional area of the plate A, and the immersion depth b:

$$F_w = p \cdot \gamma \cdot \cos\theta - \rho \cdot g \cdot A \cdot b, \tag{6}$$

where the perimeter $p = 2 \cdot (d_p + t_p)$, d_p is the plate length, t_p the plate thickness and the term $\rho \cdot g \cdot A \cdot b$ stands for the volume of liquid displaces by the plate. [5] When the end of the plate is exactly on the level of the general liquid surface (Fig. 11), the force F becomes F_o:

$$F_o = p \cdot \gamma \cdot \cos\theta. \tag{7}$$

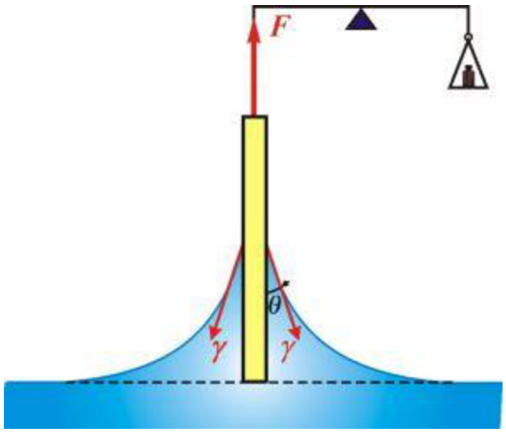

Fig. 11: Wilhelmy plate method contact angle measuring [22]

Similar to Wilhelmy plate method is a tilt plate method using a solid plate partially immersed in the liquid (Fig. 12). The tilt angle of the solid is adjusted to obtain a level liquid surface and the contact angle.

Fig. 12: Tilt plate method contact angle measurement [22]

The last one of the main measurement methods is capillary rise method where the contact angle of a liquid meniscus on a vertical flat plate is measured. See the Fig. 13 below.

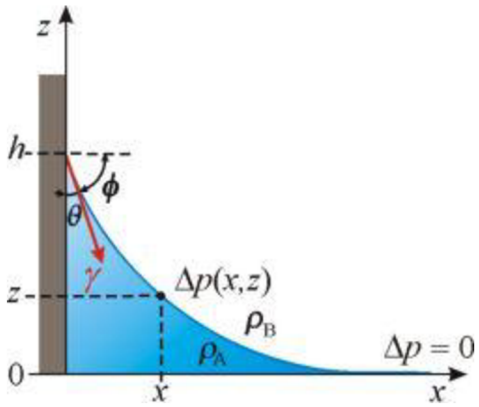

Fig. 13: Capillary rise method contact angle measurement [22]

Calculation of the contact angle comes from Young-Laplace's equation (8):

$$\sin\theta = 1 - \frac{\rho \cdot g \cdot h^2}{2 \cdot \gamma}. \tag{8}$$

Symbol h is the height of the meniscus above general liquid level.

Whether we use any of these methods there are few surface properties which affect all the measurements. First it's the surface roughness. Usually when a good wettable liquid is spread on a rough surface, the contact angle will be much lower than on a smooth one. The Young equation adjusted for rough surfaces (9) has a special constant β describing the relation between smooth and rough surface.

$$\beta \cdot \gamma_{LG} \cdot \cos\theta = \gamma_{GS} - \gamma_{LS} \tag{9}$$

Using not much wettable liquid, the affect is vice versa. The smooth surface will have lower contact angle. Second may be the absorption of liquid into the solid material. That's why the same measurement time is always important for reproducible results. The dependence of contact angle on a surface tension is included in change of Young equation to:

$$\gamma_L \cdot \cos\theta = \gamma_{S^\circ} - \left(\gamma_{S^\circ} - \gamma_{SG}\right) - \gamma_{LS}, \tag{10}$$

where the part of $\left(\gamma_{S^\circ} - \gamma_{SG}\right) = \pi$ stands for surface tension (i.e. a difference between pure solid material surface tension and its tension in equilibrium with gas phase (vapor of evaporating present liquid).

Influence of chemical inhomogeneity is also inconsiderable. If there are some inhomogeneous parts within the surface composition we consider it as two separate surfaces with different chemical structure f_A, f_B. Cassie's equation (11) describes such a change:

$$\cos\theta_S = f_A \cdot \cos\theta_A + f_B \cdot \cos\theta_B. \tag{11}$$

The summary contact angle θ_S is given by individual contact angles of both parts.

2.2.2 Surface free energy

The measurement of contact angle of liquid on a solid surface leads to description of material by surface free energy. It's a part of potential energy of surface molecules and refers to work needed for extension of the surface on a distance Δx. Generally is this energy described by equation:

$$W_s = \gamma \cdot \Delta S, \tag{12}$$

where the area extension equals to product of length of surface and the distance: $\Delta S = l \cdot \Delta x$. However, there are few ways how to calculate this energy.

First is the Fowkes theory based on suggestion that the surface free energy should be considered as a sum of independent terms, each representing a particular intermolecular force.[3] For instance, the surface energy of water (*w*) can be written as a sum of hydrogen bonding (*h*) and dispersion (*d*) forces:

$$\gamma_w = \gamma_w^h + \gamma_w^d. \tag{13}$$

But when a drop of water is put on the surface which can interact only by dispersion forces, then the Young equation becomes:

$$\gamma_w \cdot (1 + \cos\theta) = 2 \cdot \sqrt{(\gamma_w^d \cdot \gamma_S)}, \tag{14}$$

from where the solid surface free energy γ_S can be obtained. [3] Therefor this method requires only one measuring liquid.

Owens-Wendt-Kaelble theory [23] follows the Fowkes theory and adjust his equation for separated dispersion (or apolar *d*) and polar (*p*) forces into:

$$\gamma_{LS} = \gamma_S + \cdot\gamma_L - 2 \cdot \left(\sqrt{\gamma_S^d \gamma_L^d} + \sqrt{\gamma_S^p \gamma_L^p}\right). \tag{15}$$

Also the Owens-Wendt-Kaelble geometric mean method [24] can be described as:

$$(1 + \cos\theta) \cdot \gamma_L = 2 \cdot \left(\sqrt{\gamma_S^d \gamma_L^d} + \sqrt{\gamma_S^p \gamma_L^p}\right). \tag{16}$$

Then there is the Wu harmonic mean method [25] substituting the dispersion and the polar interaction terms of equation 2.14 by:

$$I^d = 2 \cdot \frac{(\gamma_S^d \gamma_L^d)}{(\gamma_S^d + \gamma_L^d)} \tag{17}$$

and

$$I^p = 2 \cdot \frac{(\gamma_S^p \gamma_L^p)}{(\gamma_S^p + \gamma_L^p)}. \tag{18}$$

The full equation seems as follows:

$$(1+\cos\theta)\cdot\gamma_L = 4\cdot\left(\frac{\gamma_S^d\gamma_L^d}{\gamma_S^d+\gamma_L^d}+\frac{\gamma_S^p\gamma_L^p}{\gamma_S^p+\gamma_L^p}\right). \tag{19}$$

For this calculation a system of two equations and two unknowns has to be solved; thus a measurement of the equilibrium contact angles of two liquids is required. Empirical observations suggest that the OWK geometric mean method is preferable for high-energy substances while the Wu harmonic method is mostly used for low-energy materials. [3]

However, in many substances other interactions appear and those cannot be predicted by the geometrical mean equation. Good, van Oss and Chaudhury [26] proposed another theory using determinations of electron-acceptor and electron-donor interactions between acids and bases (*AB*; in Lewis sense) and Lifshitz-van der Waals (*LW*) component:

$$\gamma = \gamma^{AB} + \gamma^{LW}, \tag{20}$$

where the acid-base component of bipolar material *i* is:

$$\gamma_i^{AB} = 2\cdot\sqrt{\gamma_i^+\cdot\gamma_i^-}\,. \tag{21}$$

The superscripts + and – stands for the electron-acceptor and electron-donor parameters respectively. Materials exhibiting only electron-donor or electron-acceptor properties are called monopolar, those which contain only *LW* component are called apolar and substances having both parts are called bipolar. By combination with Young equation (4) a complete expression of acid-base theory surface free energy occurs:

$$(1+\cos\theta)\cdot\gamma_L = 2\cdot\left(\sqrt{\gamma_S^{LW}\cdot\gamma_L^{LW}}+\sqrt{\gamma_S^+\cdot\gamma_L^-}+\sqrt{\gamma_S^-\cdot\gamma_L^+}\right). \tag{22}$$

Thus the three parameters characterizing the solid surface free energy and its behavior towards the surroundings can be determined by measuring the equilibrium contact angles of at least three liquids. Two of these liquids must be polar and one apolar. Also the relevant values of the surface tension components of these liquids must be known.

3 EXPERIMENTAL PART

3.1 Tested plasma polymers

Three series of tetravinylsilane (TVS) plasma polymers were measured during this research. (For depositing thin layers a TVS monomer with 97 % purity was purchased from Sigma-Aldrich Co.) All of samples were produced by plasma-enhanced chemical vapor deposition (PECVD) method. The used method is based on chemical reaction involved by additional source of energy – especially plasma. Inside reaction chamber a glow discharge occurs and causes the film deposition from monomer vapor. This process has its main advantage in using lower pressure and temperature in comparison with other types of chemical deposition methods.

Samples were produced on the *A3* device, built especially for PECVD. This vacuum apparatus works with a basic pressure of 10^{-6}–10^{-5} Pa and is controlled through special developed software controller. More details about this device can be found in [27].

First series of samples was prepared from pure TVS monomer, the second was prepared from a mixture of TVS with argon gas (Linde Gas a.s. with purity of 99.999 %) and the third from a mixture of TVS with oxygen gas (Linde Gas a.s. with purity of 99.995 %). Samples were deposited on 10 × 10 mm^2 glass substrates which were previously cleaned in an ethanol solution in ultrasonic cleaner for 10 min and argon plasma (10 sccm, 5.0 Pa, 5 W) for 10 min.

3.1.1 Deposition conditions

When talking about deposition conditions, the most important is called effective power P_{eff}. Its amount refers to time period T_p when the power is switch on/off (t_{on} and t_{off}) (23). The ratio of switching the plasma generator on and off S_p (24) multiplied the total added power P_{total} gives an amount of a power P_{eff} added to the pulsed plasma while preparing thin film (25):

$$T_p = t_{on} + t_{off} \ [\mathrm{s}], \tag{23}$$

$$S = \frac{t_{on}}{T} \cdot 100 \ [\%], \tag{24}$$

$$P_{eff} = P_{total} \cdot S. \tag{25}$$

An enhancement of the effective power causes more effective fragmentation of monomer which leads to decrease of vinyl group concentration in the layer.

Other conditions like monomer flow rate F, temperature T and pressure P was constant for every series. Monomer flow rate was adjusted at 3.8 sccm within pure TVS series and within the other series with added gas 0.3 sccm while the Argon flow rate was 3.5 sccm using the total flow rate constant at 3.8 sccm. Deposition pressure was fixed at 2.7 Pa for each series. Monomer vapor was maintained at a constant temperature of 14.6 °C.

3.2 Contact angle measurements

In connection with the theory part a sessile drop method was used for measuring contact angles. This method offers a good interpretation of data and is easily comparable with previous results of plasma polymer features measuring.

3.2.1 Used device

For measuring contact angles an OCA 25 device was used. As we can see in Fig. 14, there are 3 main parts: an eyepiece (**1**), sample stage (**2**) and injections holder (**3**). This device also requires a connection to computer with SCA 20 software (**4**) for optical evaluation of a liquid drop on surface.

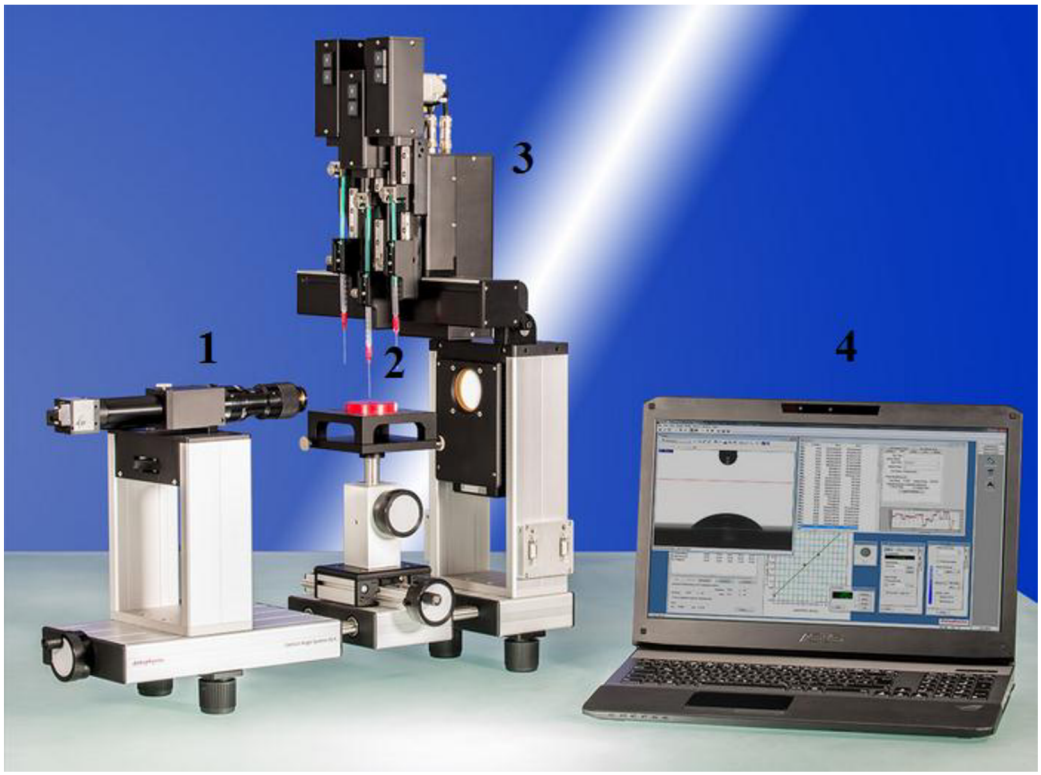

Fig. 14: The OCA 25 Contact angle measuring device [28]

After turning the apparatus on, an inside lamp illuminates an area behind the sample stand and a clear view on a drop through the eyepiece is available. A sharp contour is reached by adjusting appropriate screws.

3.2.2 Measurement procedure and calculation

During contact angle measurements there need to be at least similar conditions for each measurement because there exist variables that affect results. Those cause liquid evaporation (Fig. 15), drop vibration and other deviations.

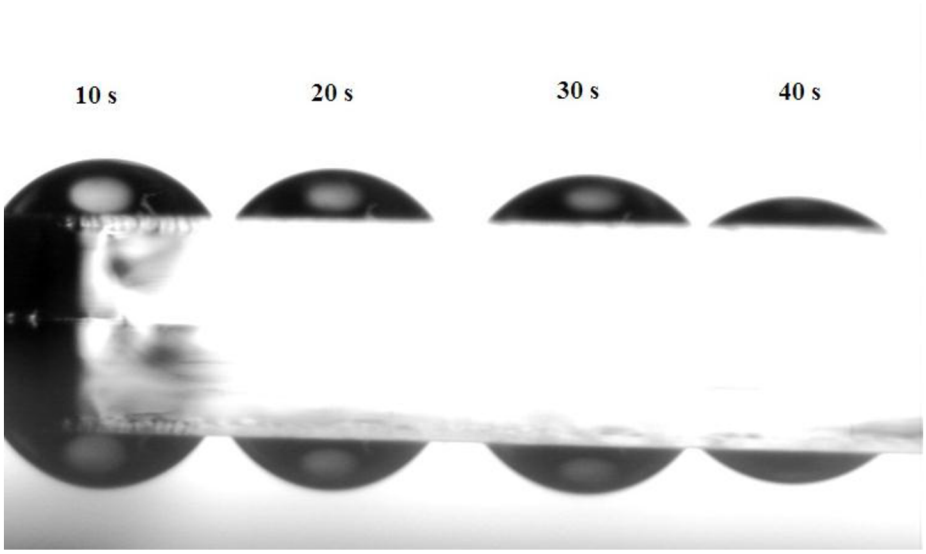

Fig. 15: A water drop evaporation during time on glass substrate

To prevent evaporation a constant time (less than 10 s), drop volume (2 μl) and temperature (varying from 23 °C to 25 °C) was used. Also a special care was taken to avoid drop vibrations.

For each of four liquids (water, diiodomethane, form amide and glycerol) 10 drops on each substrate was dripped to increase accuracy of surface free energy calculations. Those data were averaged in MS Excel (26). The standard deviation was also calculated (27) and to create a range of possible surface free energy result according to contact angle measurement error a two other values were used for surface free energy calculation – an average plus standard deviation and an average minus standard deviation.

$$\bar{\theta} = \frac{\sum_{i=1} \theta_i}{N}, \tag{26}$$

$$\sigma = \sqrt{\frac{1}{N}\sum_{i=1}^{N}\left(\theta_i - \bar{\theta}\right)^2}\,. \tag{27}$$

The surface free energy calculation was made by SCA 10 software (Fig. 16). When a method is chosen (OWK, Wu and acid-base method were used.) (**1**), the next step is to choose the test liquid from a library (**2**). It is important to follow the same surface free energy value of test liquid (**3**) in every calculation. According to [29] referenced surface free energy and its component values were chosen. They are shown in Tab. 2 for OWK method, in Tab. 3 for Wu method and in Tab. 4 for acid-base method.

Tab. 2: Surface free energy and its components values for the measuring liquids for OWK geometric mean calculation method in mJ/m^2

Measuring liquid	γ	γ^d	γ^p	Reference
Water	72.80±0.05	21.80±0.70	51.00	[30]
Diiodomethane	50.80	50.42	0.38	[31]

Tab. 3: Surface free energy and its components values for the measuring liquids for Wu harmonic mean calculation method in mJ/m^2

Measuring liquid	γ	γ^d	γ^p	Reference
Water	72.80±0.05	21.80±0.70	51.00	[30]
Diiodomethane	50.80	46.74	4.06	[31]

Tab. 4: Surface free energy and its components values for the measuring liquids for acid-base calculation method in mJ/m^2

Measuring liquid	Character	γ	γ^{LW}	γ^+	γ^-	Reference
Water	Bipolar	72.80±0.05	21.80±0.70	25.50	25.50	[32]
Diiodomethane	Apolar	50.80	50.80	0.00	0.00	[32]
Form amide	Bipolar	58.00	39.00	2.28±0.60	39.60	[33]
Glycerol	Bipolar	64.00	34.00	3.92±0.70	57.40	[33]

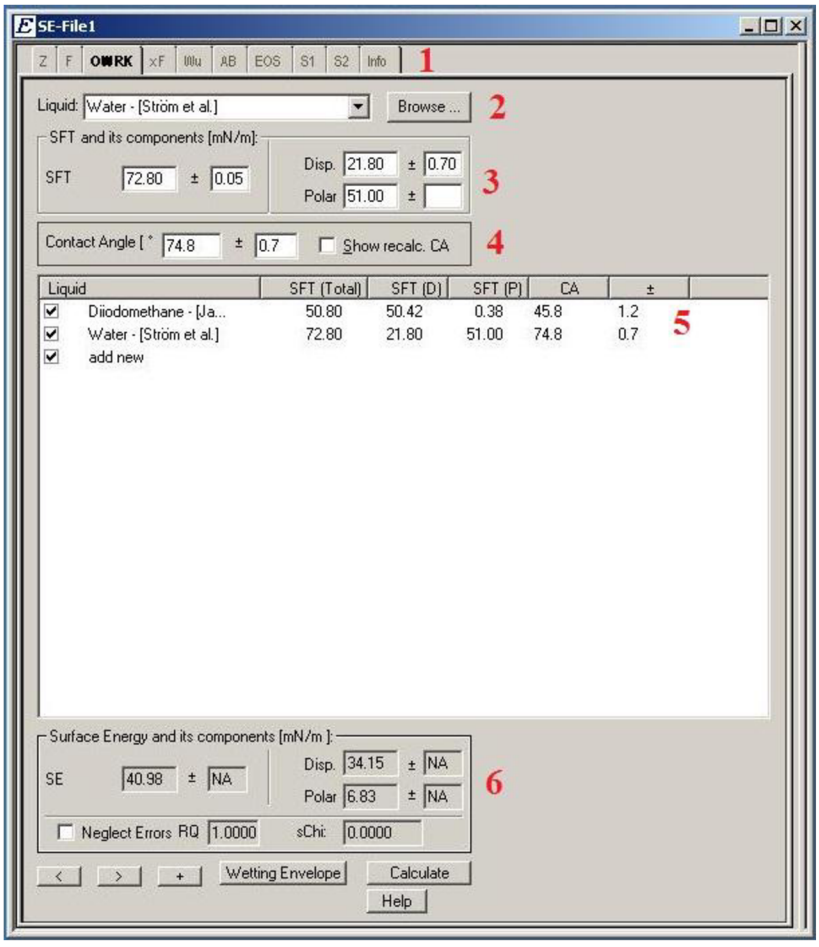

Fig. 16: A screen shot of SCA 10 software surface free energy calculation

For calculation of OWK and Wu method's results only water and diiodomethane values of contact angle and its errors were used. Calculation of acid-base method energy values were done with all of mentioned liquids.

4 RESULTS AND DISCUSSION

According to measured data a series of graphs was prepared. In first three graphs, contact angle dependence for every of measuring liquid is showed. First series of pp-TVS (plasma polymerized) film of increasing effective plasma power from 2 W to 150 W is described in Fig. 17. All of measuring liquids showed slightly decreasing contact angle dependence. Water contact angle starts at 87.50±1.54 ° and ends at 83.92±1.11 °. Diiodomethane goes from 40.82±0.83 ° to 34.20±1.93 °. Form amide has its maximum at 69.90±1.73 ° and its minimum at 62.50±0.89 °. And glycerol varies from 74.97±0.96 ° to 67.48±5.70 °.

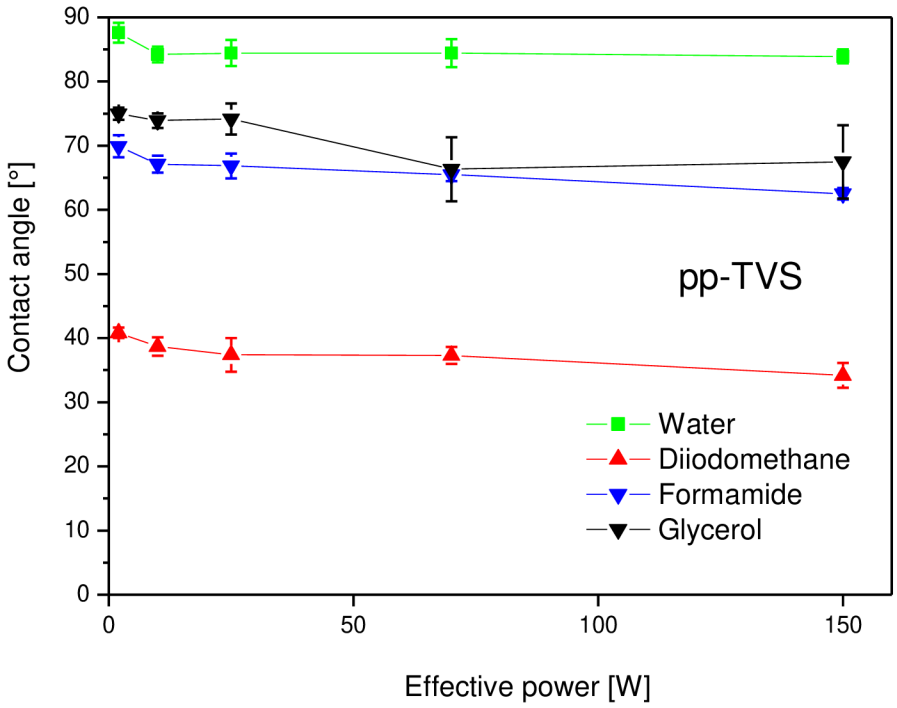

Fig. 17: Contact angles dependence of pp-TVS film

The dependency of contact angles in second series (pp-TVS/Ar) can be seen in Fig. 18. It also shows a little decrease or approximately constant dependence but values of angles are a little bit lower in comparison with pp-TVS series. Water angle maximum and minimum: 83.75±0.85 °, 76.01±1.48 °. Diiodomethane: 35.60±1.78 °, 36.29±0.88 °. Form amide: 64.50±1.14 °, 55.42±2.01 °. Glycerol: 71.39±1.37 ° and 59.06±7.00 °.

The third series of pp-TVS/O_2 contact angles are shown in Fig. 19. There is a noticeable decrease in the beginning for every measuring liquid. Water angle maximum and minimum: 50.18±2.98 °, 16.36±3.39 °. Diiodomethane: 42.37±2.06 °, 37.12±2.14 °. Form amide: 33.74±0.74 °, 12.4±1.20 °. Glycerol: 46.20±1.47 ° and 13.51±1.26 °.

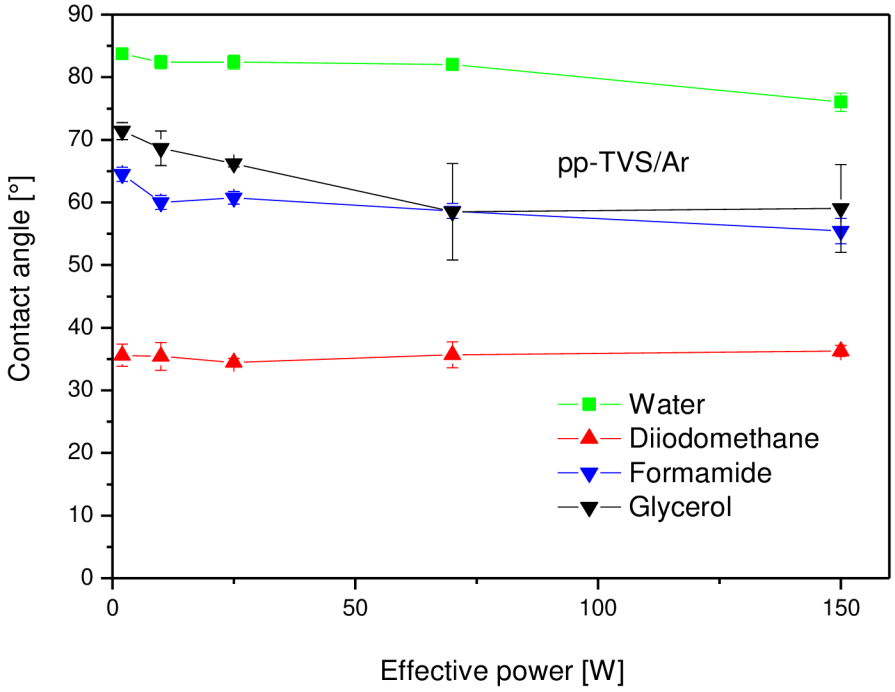

Fig. 18: Contact angles dependence of pp-TVS/Ar film

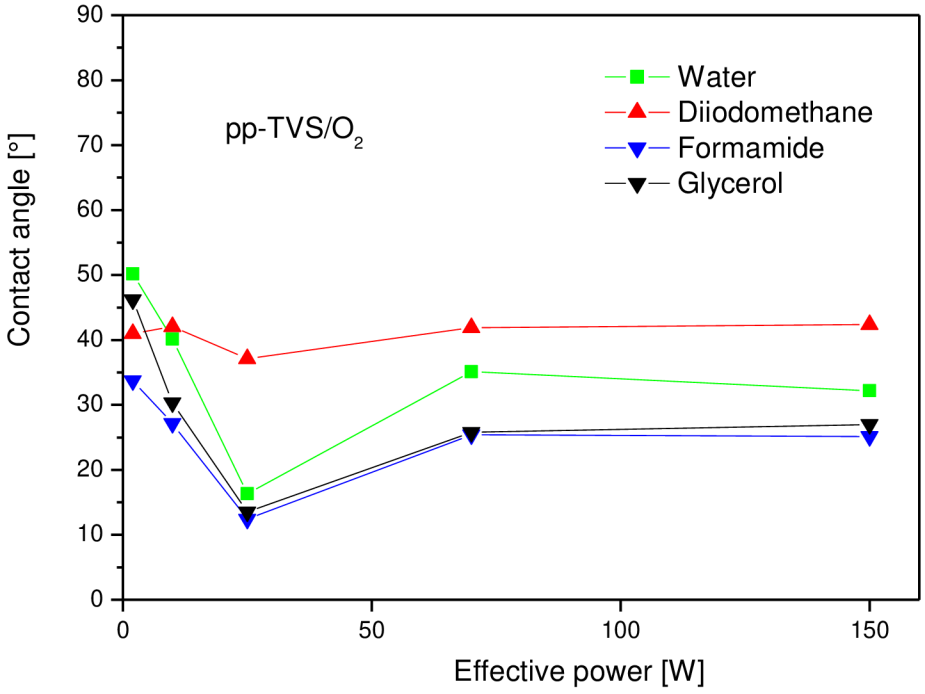

Fig. 19: Contact angles dependence of pp-TVS/O_2 film

After calculation of surface free energy and its components by OWK geometric method another three graphs were made. In Fig. 20 a dependence of total energy γ, electron donor energy part γ^- and electron acceptor energy part γ^+ is showed for pp-TVS film series. The total surface free energy starts at 39.74±0.49 mJ/m^2 and rises up to 43.18±0.78 mJ/m^2. It is a sum of nearly constant 2±0.35 mJ/m^2 polar component and dispersion one ranging from 38.10±0.30 mJ/m^2 to 41.08±0.79 mJ/m^2.

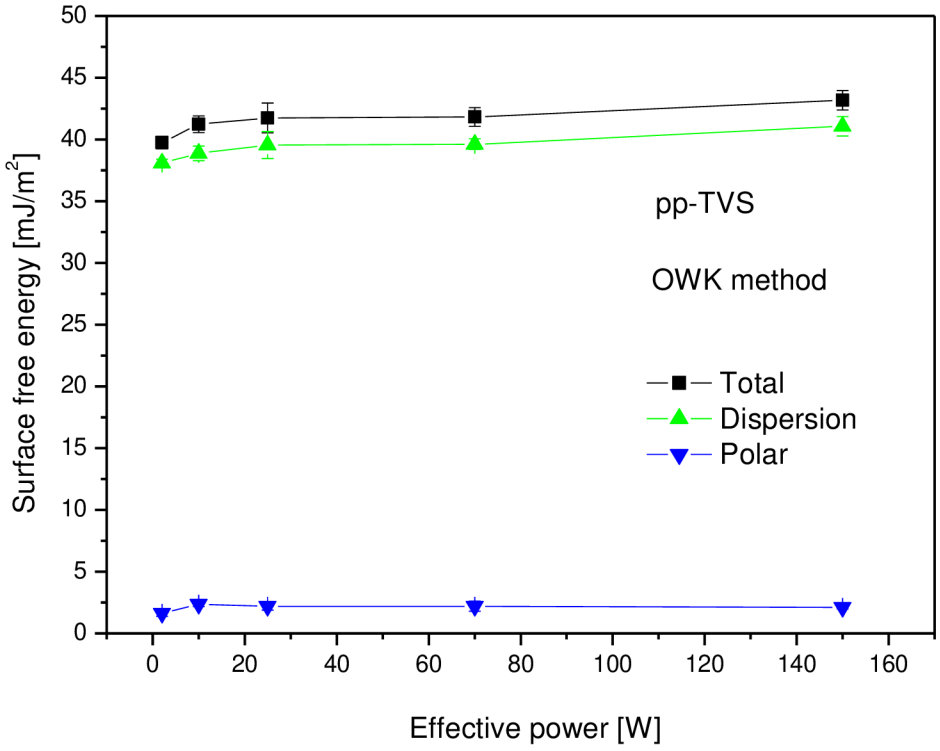

Fig. 20: OWK method surface free energy components dependence of pp-TVS

Results of OWK method calculation for pp-TVS/Ar is are in Fig. 21. There is a slightly increase of total surface free energy by the sample of effective power 150 W but with taking account of the error deviations it is still constant. Its approximately value is 43.34±0.70 mJ/m^2. Disperse component varies between 39.26±0.29 mJ/m^2 and 40.80± 0.20 mJ/m^2, and polar component is about 2.24±0.09.

Data of pp-TVS/O_2 series are in Fig. 22. As we can see, there is a rise within 25 W sample due to increase in polar energy component. Total surface free energy values rise from 57.29±3.67 mJ/m^2 to 64.91±0.71 mJ/m^2 (except 25 W sample energy which is 64.91±0.71 mJ/m^2). Dispersion components stay around 33.41±0.48 mJ/m^2. Polar component values 20.36±1.27 mJ/m^2–37.54±0.35 mJ/m^2.

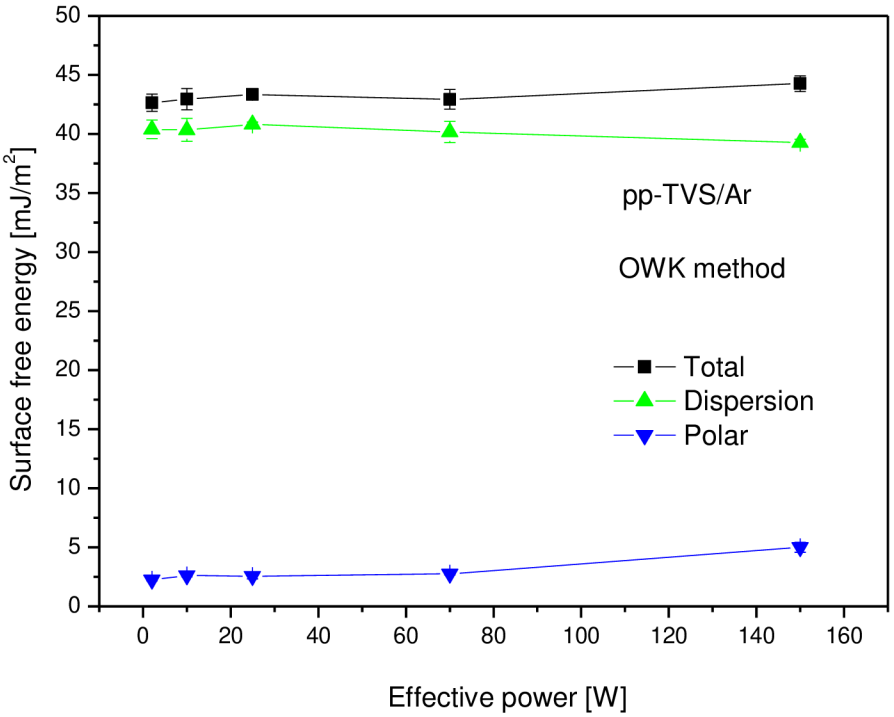

Fig. 21: OWK method surface free energy components dependence of pp-TVS/Ar

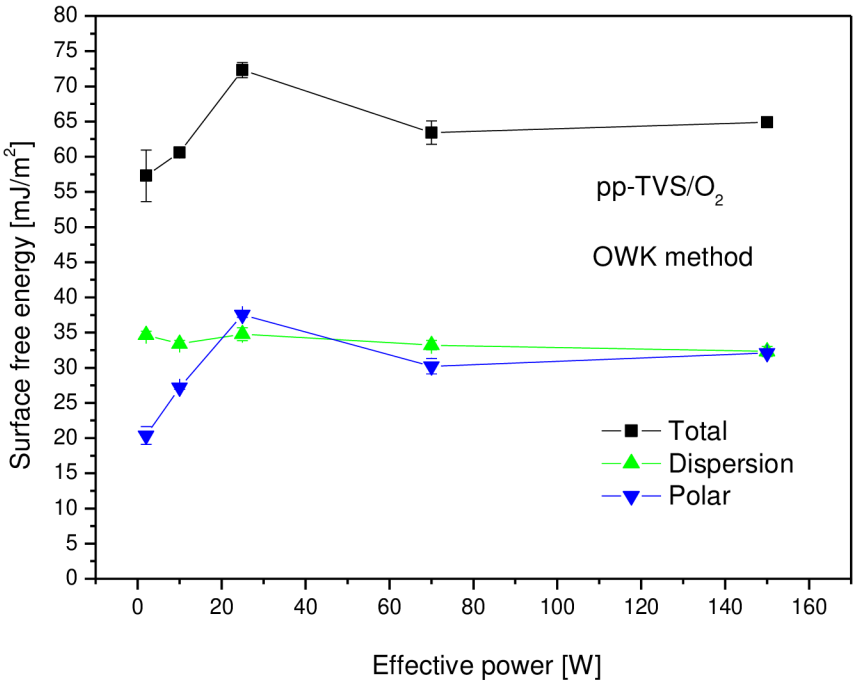

Fig. 22: OWK method surface free energy components dependence of pp-TVS/O_2

Wu harmonic method calculation results are shown below in Fig. 23, Fig. 24, Fig. 25. The first figure describes values of first series with pure TVS monomer. Total energy (as a sum of its components) rises from 40.79±0.56 mJ/m^2 to 44.16±0.78 mJ/m^2. Disperse part follows the tendency from 34.38±0.11 mJ/m^2 to 36.78±0.62 mJ/m^2. Polar part stays approximately constant at 7.21±0.46 mJ/m^2.

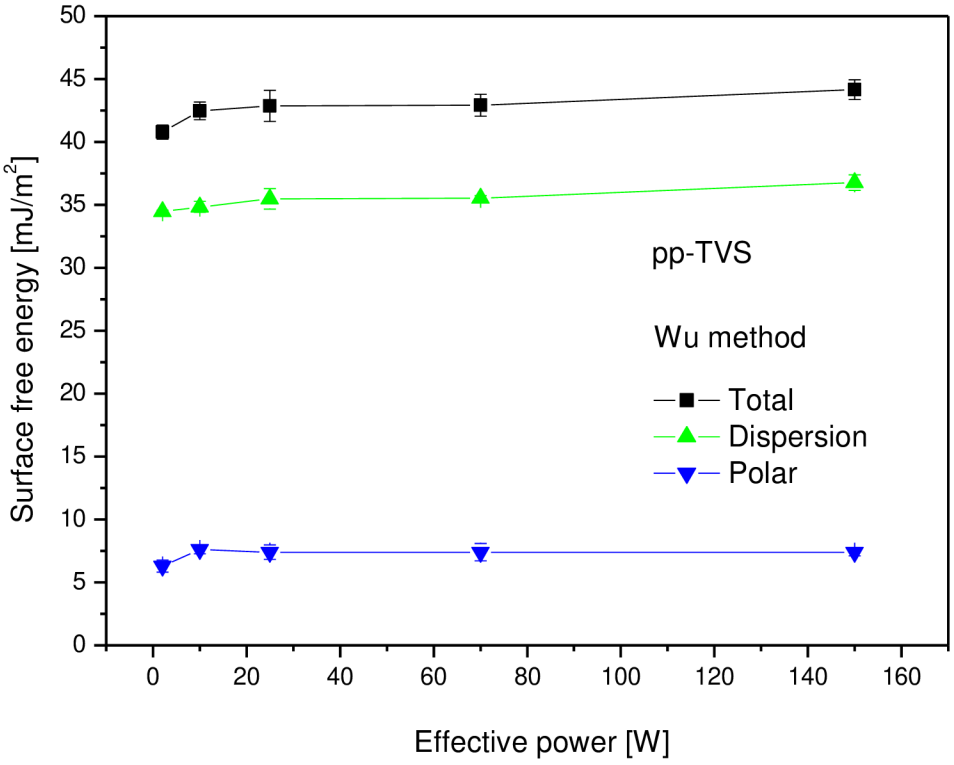

Fig. 23: Wu method surface free energy components dependence of pp-TVS

The pp-TVS/Ar series has a similar process (Fig. 24). Total energy here goes from 43.70±0.71 mJ/m^2 to 46.04±0.71 mJ/m^2, dispersion part drops a very little from 36.15±0.64 mJ/m^2 to 34.82±0.22 mJ/m^2 and on the other hand, polar part rises from 7.55±0.19 mJ/m^2 to 11.22±0.52 mJ/m^2. The dependence seems quite as the previous with the difference in the last sample of 150 W P_{eff} where the ratio between disperse and polar part is slightly different – in Argon series polar part rises a little.

Values for pp-TVS/O_2 series (Fig. 25) rise from 61.86±1.67 mJ/m^2 over 77.57±1.22 mJ/m^2 to 70.31±0.86 mJ/m^2. Dispersion component stays about 38.34±0.78 mJ/m^2. Polar component shows a little increase (similar to the OWK polar component) at 25 W - 37.1±0.52 mJ/m^2. It starts at 23.1±1.09 mJ/m^2 and ends at 32.19±0.09 mJ/m^2.

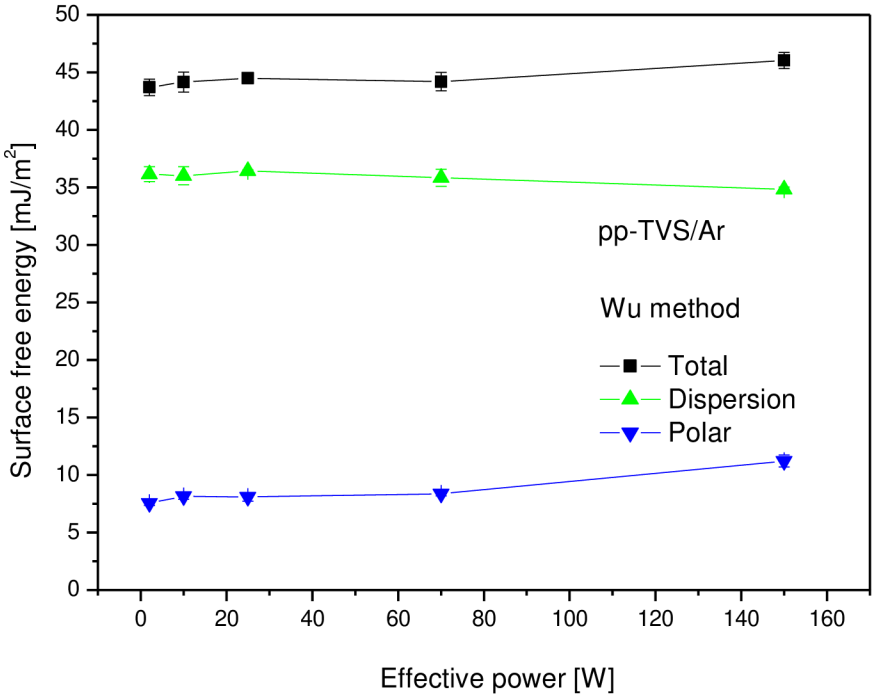

Fig. 24: Wu method components dependence of pp-TVS/Ar

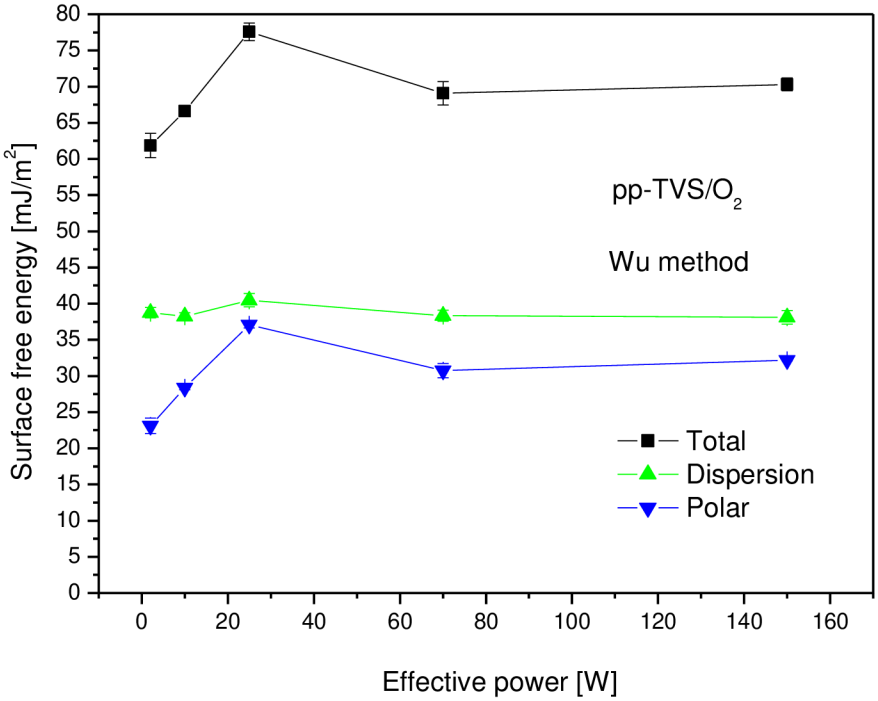

Fig. 25: Wu method components dependence of pp-TVS/O_2

Acid-base method (AB) calculations have been processed into following graphs. Fig. 26 describes total surface free energy γ with acid γ^+ (electron acceptor like), base γ^- (electron donor like) and Lifshitz-van der Waals γ^{LW} component of pure TVS series. Total energy rises from 39.05±0.36 mJ/m^2 to 41.34±0.68 mJ/m^2. The Lifshitz-van der Waals component (LW) values are equal. Electron donor (in a graph called base) component varies between 2.69±0.46 mJ/m^2 and 3.95±0.42 mJ/m^2. Acid component is zero within all samples.

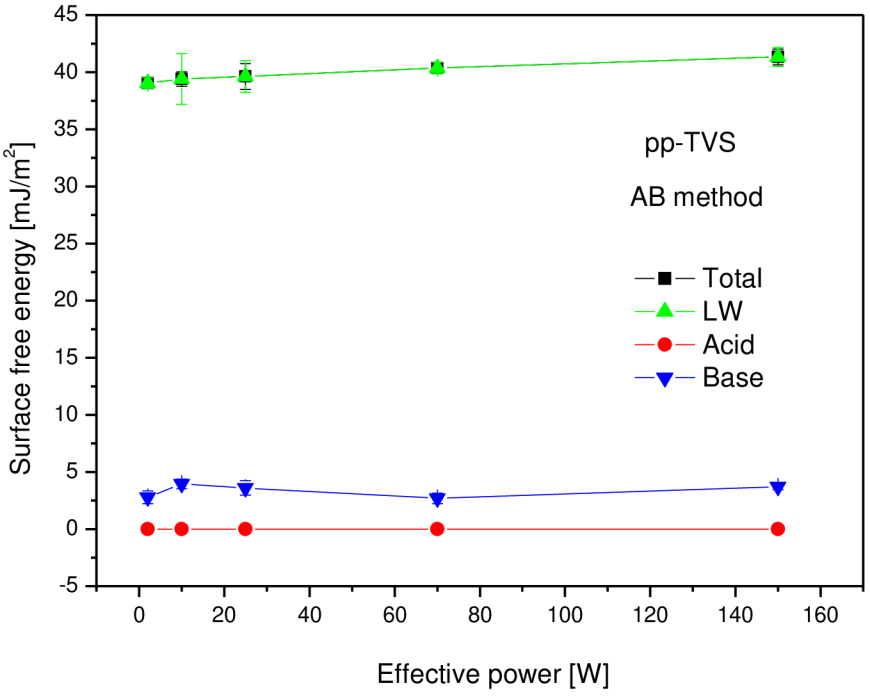

Fig. 26: AB method surface free energy components dependence of pp-TVS

Dependence of AB energy components of TVS + Argon series are showed in Fig. 27. Total energy rises slightly from 40.66±0.78 mJ/m^2 to 42.60±0.91 mJ/m^2. LW component also rises, but does not equal total energy; it is a little lower due to increasing base component. LW: 40.66±0.96 mJ/m^2–41.41±0.42 mJ/m^2. Base: 4.14±0.18 mJ/m^2–7.79±0.18mJ/m^2. Even acid component was observed in this calculation results but just with negligible values around 0.06±0.04 mJ/m^2.

Pp-TVS/O_2 total energy value increases at the beginning due to a rise within base (el. donor) component which showed up at a 25 W sample (Fig. 28). Its total energy value is 60.86±0.17 mJ/m^2. Except that it goes from 49.38±0.56 mJ/m^2 to 55.71±1.52 mJ/m^2. LW component is 39.11±0.73 mJ/m^2–37.81±1.12 mJ/m^2. Its aximum is 40.50±0.99 mJ/m^2. Acid component is nearly constant with value of 2.27±0.16 mJ/m^2. Base component varies from 25.16±3.03 mJ/m^2 to 38.08±1.39 mJ/m^2. Its maximum has 45.31±1.86 mJ/m^2.

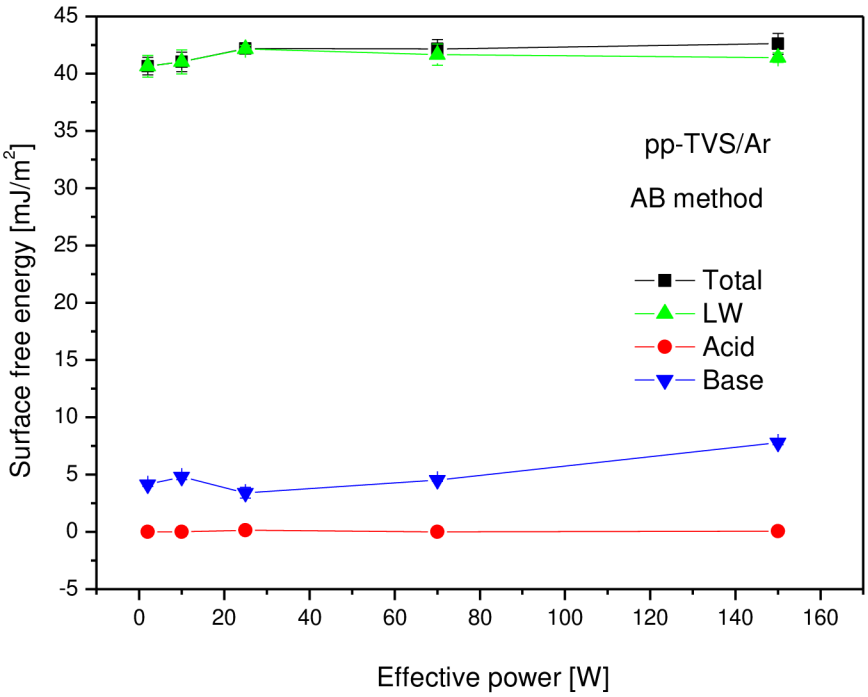

Fig. 27: AB method surface free energy components dependence of pp-TVS/Ar

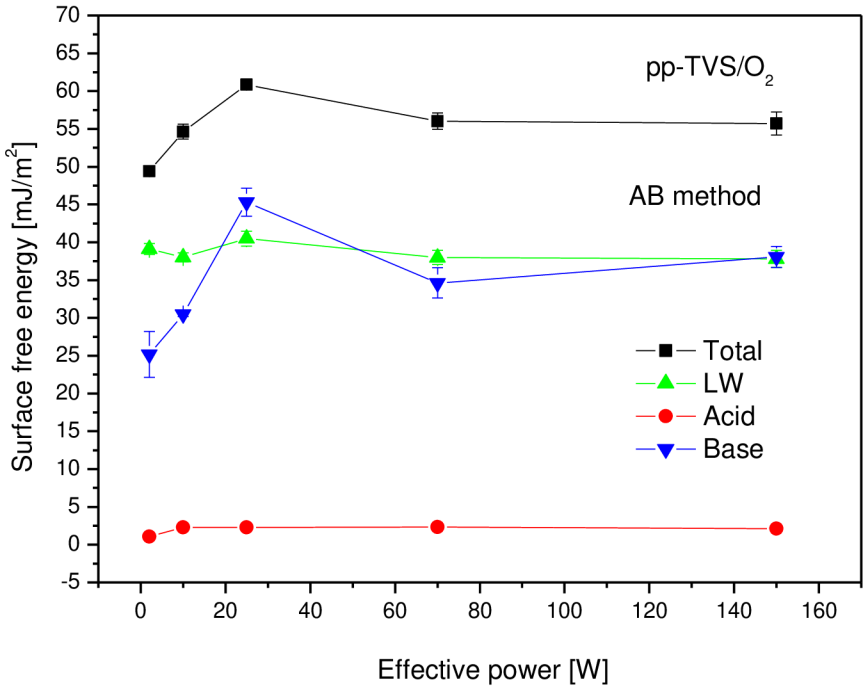

Fig. 28: AB method surface free energy components dependence of pp-TVS/O_2

To summarize all three method's results into simple graphs Fig. 29, Fig. 30 and Fig. 31 were made. Measurements and calculations of both series showed a slightly increasing dependence of surface free energy on the effective power, no matter which method was used. Highest values belong to Wu harmonic mean method. In the middle results from OWK geometric mean method can be found and the lowest values describe acid-base method results.

It seems that with increasing effective power also a surface free energy rises but very slightly. It might be caused by decreasing concentration of vinyl groups inside rising layer. Added energy ionize plasma state polymer and gas thus a concentration of ions, electron and radicals grows and the polymer gets more and more fragmented. With continuing fragmentation a less vinyl groups occur and the wettability together with surface free energy increases. [34]

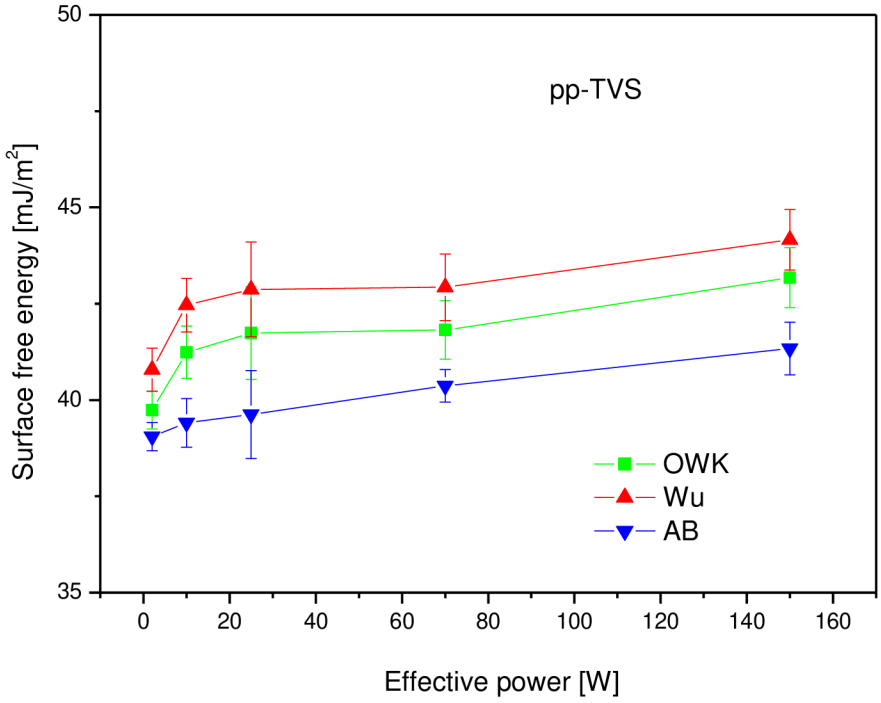

Fig. 29: Surface free energy dependence of pp-TVS

Within pp-TVS/O_2 an undefined dependence was observed. It might be caused by some error which occurred during preparation (so there may be more oxygen than was meant to be).

Generally, the surface free energy of pp-TVS/O_2 series is much higher due to its high polar components because it contains –OH and –C=O groups which affect wettability. [35]

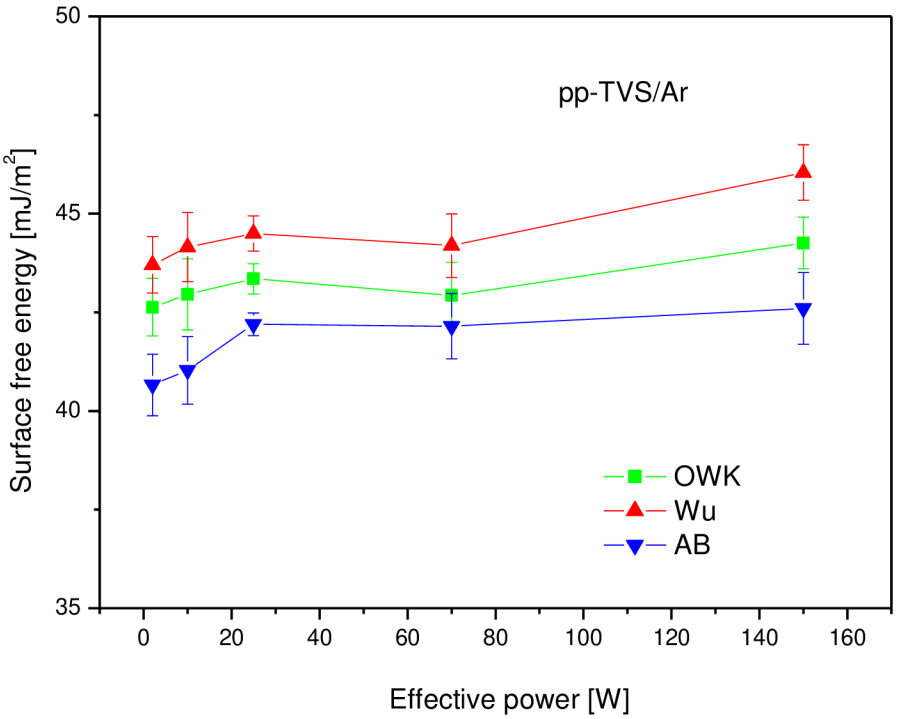

Fig. 30: Surface free energy dependence of pp-TVS/Ar

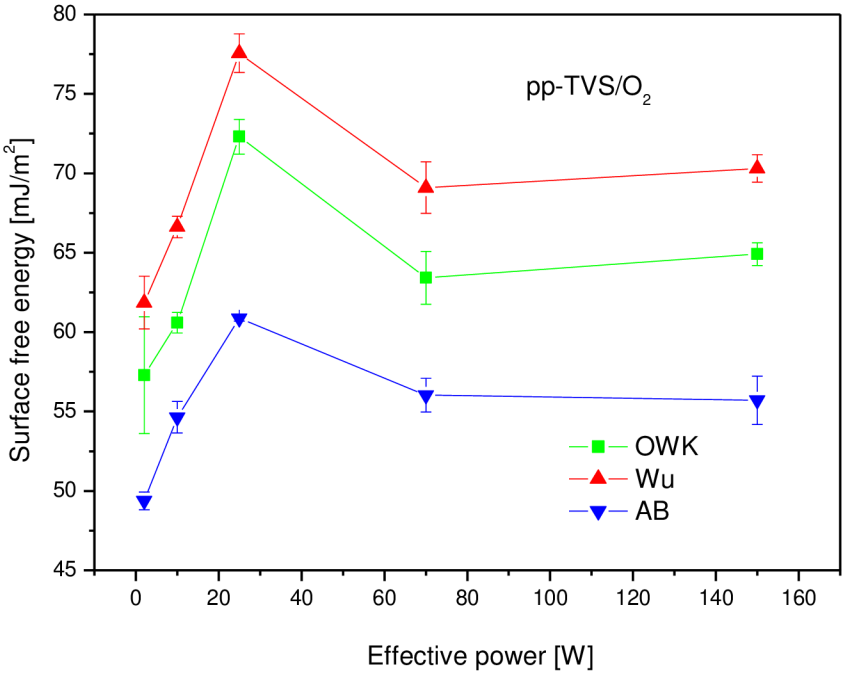

Fig. 31: Surface free energy dependence of pp-TVS/O_2

5 CONCLUSION

Thin films of plasma polymers, especially those prepared from organosilicons, are nowadays widely researched among material chemistry scientists for their promising features and possibilities of varying their features by deposition conditions.

This thesis focus on thin film plasma polymer contact angle measurement and calculation of surface free energy by three different methods – OWK, Wu and acid-base method. Thus three series of thin film plasma polymers by PECVD method on a glass substrate were made. Those are pp-TVS, pp-TVS/Ar and pp-TVS/O_2. Each series contained five samples prepared with increasing effective power by 2, 10, 25, 70 and 150 W. Contact angles of four measuring liquids (water, diiodomethane, form amide and glycerol) by the sessile drop method were measured on OCA 10 device. Then surface free energy values by OWK, Wu and acid-base methods were calculated on SCA 10 software for comparison.

The total surface free energy of both pp-TVS and pp-TVS/Ar series showed a slightly increasing dependence on effective power they were made by. Values of pp-TVS varied in the range 39–43 mJ/m^2 for OWK method, 40–44 mJ/m^2 for Wu method and 39–41 mJ/m^2 for acid-base method calculation. Second series of pp-TVS/Ar showed a little higher energy values: 43–44 mJ/m^2 for OWK, 44–46 mJ/m^2 for Wu and 41–43 mJ/m^2 for acid-base method calculation. Total surface free energy of pp-TVS/O_2 samples rises up and then drops. OWK method results goes from 57 mJ/m^2 over 72 mJ/m^2 to 65 mJ/m^2. Wu method result starts at 62 mJ/m^2, rises up to 78 mJ/m^2 and drops again to 70 mJ/m^2. Acid-base method values begin at 49 mJ/m^2, reach 61 mJ/m^2 and decrease to 56 mJ/m^2. There is a possibility of production error within a 25 W sample which showed the maximum value but it has not been proved yet. It might be the aim of another study of chemical structure inside plasma polymerized thin film.

Generally a quite increasing dependence of surface free energy on deposition conditions were observed within all calculation method's results. The dependence is more distinct for pp-TVS and pp-TVS/Ar than pp-TVS/O_2 series but the thin film polymer prepared in a mixture with oxygen showed at least the highest values of free surface energy.

6 LIST OF SOURCES

[1] FREUND, L. a S. SURESH *Thin Film Materials: Stress, Defect Formation and Surface Evolution* [online]. Cambridge University Press, 2003 [cit. 2015-11-30]. ISBN 0-521-82281-5. Dostupné z: https://books.google.cz/books?id=9UNnzNYAkboC&lpg=PP1&dq=thin%20film&hl=cs&pg=PR4#v=onepage&q=thin%20film&f=false

[2] KIM, Jang-Kyo a Yiu-Wing MAI. *Engineered interfaces in fiber reinforced composites*. 1st ed. Amsterdam: Elsevier, 1998, 401 s. ISBN 0080426956.

[3] GARBASSI, F, Marco MORRA a E OCCHIELLO. *Polymer surfaces: from physics to technology*. Rev. and updated ed. New York: Wiley, c1998, ix, 486 p. ISBN 04-719-7100-6.

[4] INAGAKI, N. *Plasma surface modification and plasma polymerization*. Lancaster: Technomic Publishing Company, 1996, 265 s. ISBN 1566763371.

[5] WU, Souheng. *Polymer interface and adhesion*. New York: M. Dekker, c1982, xiii, 630 p. ISBN 08-247-1533-0.

[6] CECH, Vladimir, Josef ZEMEK a Vratislav PERINA. Chemistry of Plasma-Polymerized Vinyltriethoxysilane Controlled by Deposition Conditions. *Plasma Processes and Polymers* [online]. Weinheim: WILEY-VCH Verlag, 2008, **5**(8), 745-752 [cit. 2016-02-11]. DOI: 10.1002/ppap.200800007. ISSN 16128850. Dostupné z: http://onlinelibrary.wiley.com.ezproxy.lib.vutbr.cz/doi/10.1002/ppap.200800007/full

[7] SEGUI, Yvan. Plasma deposition from organosilicon monomers. In: D' AGOSTINO, R. (ed.) *Plasma processing of polymers*. Netherlands: Kluwer Academic Publishers, 1997, s. 305-319. ISBN 0-7923-4859-1.

[8] SEGUI, Y. a Bui AI. Gas discharge in hexamethyldisiloxane. *Journal of Applied Polymer Science* [online]. 1976, **20**(6), 1611-1618 [cit. 2016-05-03]. DOI: 10.1002/app.1976.070200618. ISSN 00218995. Dostupné z: http://doi.wiley.com/10.1002/app.1976.070200618

[9] WRÓBEL, A., M. WERTHEIMER, J. DIB a H. SCHREIBER Polymerization of Organosilicones in Microwave Discharges. *Journal of Macromolecular Science: Part A - Chemistry* [online]. 2006, **14**(3), 321-337 [cit. 2016-05-03]. DOI: 10.1080/00222338008056716. ISSN 0022-233x. Dostupné z: http://www.tandfonline.com/doi/abs/10.1080/00222338008056716

[10] TAJIMA, Ichiro a Minoru YAMAMOTO. Spectroscopic study on chemical structure of plasma-polymerized hexamethyldisiloxane. *Journal of Polymer Science: Polymer Chemistry Edition* [online]. 1985, **23**(3), 615-622 [cit. 2016-05-03]. DOI: 10.1002/pol.1985.170230303. ISSN 03606376. Dostupné z: http://doi.wiley.com/10.1002/pol.1985.170230303

[11] AKOVALI, G. a N. HASIRCI Polymerization of hexamethyldisiloxane by plasma on activated charcoal: Investigation of parameters. *Journal of Applied Polymer Science* [online]. 1984, **29**(8), 2617-2625 [cit. 2016-03-21]. DOI: 10.1002/app.1984.070290816. ISSN 00218995. Dostupné z: http://doi.wiley.com/10.1002/app.1984.070290816

[12] SACHDEV, Krishna a Harbans SACHDEV Characterization of plasma-deposited organosilicon thin films. *Thin Solid Films* [online]. 1983, **107**(3), 245-250 [cit. 2016-03-21]. DOI: 10.1016/0040-6090(83)90403-0. ISSN 00406090. Dostupné z: http://linkinghub.elsevier.com/retrieve/pii/0040609083904030

[13] MUKHERJEE, S.P. a P.E. EVANS The deposition of thin films by the decomposition of tetra-ethoxy silane in a radio frequency glow discharge. *Thin Solid Films* [online]. 1972, **14**(1), 105-118 [cit. 2016-03-21]. DOI: 10.1016/0040-6090(72)90373-2. ISSN 00406090. Dostupné z: http://linkinghub.elsevier.com/retrieve/pii/0040609072903732

[14] PAI, C. Electron Cyclotron Resonance Microwave Discharge for Oxide Deposition Using Tetraethoxysilane. *Journal of The Electrochemical Society* [online]. 1992, **139**(3), 850- [cit. 2016-03-21]. DOI: 10.1149/1.2069315. ISSN 00134651. Dostupné z: http://jes.ecsdl.org/cgi/doi/10.1149/1.2069315

[15] SELAMOGLU, Nur. Silicon oxide deposition from tetraethoxysilane in a radio frequency downstream reactor: Mechanisms and step coverage. *Journal of Vacuum Science* [online]. 1989, **7**(6), 1345- [cit. 2016-03-21]. DOI: 10.1116/1.584536. ISSN 0734211x. Dostupné z: http://scitation.aip.org/content/avs/journal/jvstb/7/6/10.1116/1.584536

[16] ISHII, Keisuke, Yoshimichi OHKI a Hiroyuki NISHIKAWA. Optical characteristics of SiO2 formed by plasma-enhanced chemical-vapor deposition of tetraethoxysilane. *Journal of Applied Physics* [online]. 1994, **76**(9), 5418- [cit. 2016-03-21]. DOI: 10.1063/1.357196. ISSN 00218979. Dostupné z: http://scitation.aip.org/content/aip/journal/jap/76/9/10.1063/1.357196

[17] INAGAKI, N., S. KONDO a T. MURAKAMI Preparation of siloxane-like films by glow discharge polymerization. *Journal of Applied Polymer Science* [online]. 1984, **29**(11), 3595-3605 [cit. 2016-03-21]. DOI: 10.1002/app.1984.070291133. ISSN 00218995. Dostupné z: http://doi.wiley.com/10.1002/app.1984.070291133

[18] RAU, Christiane a Wilhelm KULISCH. Mechanisms of plasma polymerization of various silico-organic monomers. *Thin Solid Films* [online]. 1994, **249**(1), 28-37 [cit. 2016-03-21]. DOI: 10.1016/0040-6090(94)90081-7. ISSN 00406090. Dostupné z: http://linkinghub.elsevier.com/retrieve/pii/0040609094900817

[19] NGUYEN, V. Plasma Organosilicon Polymers. *Journal of The Electrochemical Society* [online]. 1985, **132**(8), 1925- [cit. 2016-03-21]. DOI: 10.1149/1.2114255. ISSN 00134651. Dostupné z: http://jes.ecsdl.org/cgi/doi/10.1149/1.2114255

[20] INAGAKI, N., S. KONDO, M. HIRATA a H. URUSHIBATA Plasma polymerization of organosilicon compounds. *Journal of Applied Polymer Science* [online]. 1985, **30**(8), 3385-3395 [cit. 2016-03-21]. DOI: 10.1002/app.1985.070300821. ISSN 00218995. Dostupné z: http://doi.wiley.com/10.1002/app.1985.070300821

[21] BARTOVSKÁ, Lidmila a Marie ŠIŠKOVÁ. *Fyzikální chemie povrchů a koloidních soustav*. 2. přepr.vyd. Praha: VŠCHT, 1996, 134 s. ISBN 8070802529.

[22] BARTOVSKÁ, Lidmila a Marie ŠIŠKOVÁ. *Co je co v povrchové a koloidní chemii: výkladový slovník* [online]. VŠCHT Praha, 2005 [cit. 2016-02-16]. Dostupné z: http://147.33.74.135/knihy/uid_es-001/

[23] OWENS, D. a R. WENDT Estimation of the surface free energy of polymers. *Journal of Applied Polymer Science*. 1969, **13**(8), 1741-1747. DOI: 10.1002/app.1969.070130815. ISSN 00218995. Dostupné také z: http://doi.wiley.com/10.1002/app.1969.070130815

[24] KAELBLE, D. Dispersion-Polar Surface Tension Properties of Organic Solids. *The Journal of Adhesion* [online]. 2008, **2**(2), 66-81 [cit. 2016-02-25]. DOI: 10.1080/0021846708544582. ISSN 0021-8464. Dostupné z: http://www.tandfonline.com/doi/full/10.1080/0021846708544582

[25] WU, Souheng. Calculation of interfacial tension in polymer systems. *Journal of Polymer Science Part C: Polymer symposium*. 1971, (34), 19-30. ISSN 0360-8905.

[26] VAN OSS, Carel, Manoj CHAUDHURY a Robert GOOD Interfacial Lifshitz-van der Waals and polar interactions in macroscopic systems. *Chemical Reviews*. 1988, **88**(6), 927-941. DOI: 10.1021/cr00088a006. ISSN 0009-2665. Dostupné také z: http://pubs.acs.org/doi/abs/10.1021/cr00088a006

[27] BRÁNECKÝ, Martin. *Tenké vrstvy připravené v RF doutnavém výboji a jejich fyzikálně - chemické vlastnosti*. Brno, 2015. Diplomová práce. Vysoké učení technické v Brně, Fakulta elektrotechniky a komunikačních technologií. Vedoucí práce Prof. RNDr. Vladimír Čech, Ph.D.

[28] *DataPhysics: Understanding Interfaces* [online]. Filderstadt: DataPhysics Instruments GmbH, 2016 [cit. 2016-04-26]. Dostupné z: http://www.dataphysics.de

[29] Surface-free energy of silicon-based plasma polymer films. *Silanes and other coupling agents*. 1. Leiden: VSP, 2009, s. 333-348. ISBN 9789004165915.

[30] STRÖM, Göran, Monica FREDRIKSSON a Per STENIUS. Contact angles, work of adhesion, and interfacial tensions at a dissolving Hydrocarbon surface. *Journal of Colloid and Interface Science* [online]. 1987, **119**(2), 352-361 [cit. 2016-05-03]. DOI: 10.1016/0021-9797(87)90280-3. ISSN 00219797. Dostupné z: http://linkinghub.elsevier.com/retrieve/pii/0021979787902803

[31] JAńCZUK, Bronisław a Tomasz BIAŁLOPIOTROWICZ. Surface free-energy components of liquids and low energy solids and contact angles. *Journal of Colloid and Interface Science* [online]. 1989, **127**(1), 189-204 [cit. 2016-05-03]. DOI: 10.1016/0021-9797(89)90019-2. ISSN 00219797. Dostupné z: http://linkinghub.elsevier.com/retrieve/pii/0021979789900192

[32] BIRDI, K. *Handbook of surface and colloid chemistry*. 2nd ed. Boca Raton, Fla.: CRC Press, c2003. ISBN 0849310792.

[33] VAN OSS, C.J, L JU, M.K CHAUDHURY a R.J GOOD. Estimation of the polar parameters of the surface tension of liquids by contact angle measurements on gels. *Journal of Colloid and Interface Science* [online]. 1989, **128**(2), 313-319 [cit. 2016-05-03]. DOI: 10.1016/0021-9797(89)90345-7. ISSN 00219797. Dostupné z: http://linkinghub.elsevier.com/retrieve/pii/0021979789903457

[34] CECH, V., J. STUDYNKA, N. CONTE a V. PERINA Physico-chemical properties of plasma-polymerized tetravinylsilane. *Surface & Coatings Technology* [online]. Elsevier B.V, 2007, **201**(9), 5512-5517 [cit. 2016-05-13]. DOI: 10.1016/j.surfcoat.2006.07.086. ISSN 02578972.

[35] CECH, Vladimir, Jan STUDYNKA, Filip JANOS a Vratislav PERINA. Influence of Oxygen on the Chemical Structure of Plasma Polymer Films Deposited from a Mixture of Tetravinylsilane and Oxygen Gas. *Plasma Processes and Polymers* [online]. Weinheim: WILEY-VCH Verlag, 2007, **4**(1), 776-780 [cit. 2016-05-13]. DOI: 10.1002/ppap.200731903. ISSN 16128850.

7 LIST OF ABBREVIATIONS AND SYMBOLS

M ..... monomer

M_i• ..... monomer radical

•M_i•..... monomer biradical

$M_{i/k}$-M• .....longer chain monomer radical

•M_k-M• .....longer chain monomer biradical

G.....Gibbs free energy

T.....temperature

H.....enthalpy

W.....plasma supplying energy

F ..... monomer flow rate

M.....molecular weight

HMDSO .....hexamethyldisiloxane

TEOS..... tetraethoxysilane

TMDSO..... tetramethyldisiloxane

DVTMDSO ...divinyltetramethyldisiloxane

TMOS.....methyltrimethoxysilane

HMDS .....hexamethyldisilane

TMS..... tetramethylsilane

TVS .....tetravinylsilane

W_c .....work of cohesion

γ .....surface tension

$\gamma_{A/B}$ ..... surface tension of phase *A/B*

γ_{AB} .....surface tension of interface *AB*

W_a .....work of adhesion

θ.....contact angle

γ_{LG}..... liquid-gas interface surf. tension

γ_{SG}.....solid-gas interface surf. tension

γ_{LS} ..... liquid-solid interface surf. tension

F_w ..... force used for balancing W. plate

F_o.. standard force used to balance plate

p .....perimeter of measured plate

ρ .....density

b ..... immersion depth

g .....the gravitational acceleration

A ... the cross-sectional area of the plate

d_p .....plate length

t_p.....plate thickness

h ..... height

β ..... Young equation constant

γ_{S° ..... pure solid material surf. tension

$f_{A/B}$ .....chemical structure of phase *A/B*

W_s .....surface free energy

ΔS.....surface extension

l ..... length

Δx .....surface extension

OWK.....Owens-Wendt-Kaelble

γ^d .....dispersion/apolar surf. energy

γ^p ..... polar surf. energy

γ^{AB}.....acid-base energy component

γ^{LW}.....

Lifshitz-van den Waals surf. energy component

PECVD .....
plasma-enhanced chemical vapor deposition

P .....pressure

t_{on}.....time of switched on generator

t_{off}.....tome of switched off generator

T_p ..... generator switching period

S_p..... on/off time ratio of generator

P_{eff}.....effective power

P_{total}..... total added power

sccm.....standard cubic centimeter per minute

$\overline{\theta}$ ..... average contact angle

σ.....standard error

γ^+.....acid (el. aceptor) energy component

γ^-.....base (el. donor) energy component

LW..... Lifshitz-van der Waals